

Evolution of Structure in a Graft Copolymer-Homopolymer Blend under Strain

M. Rabeony* and D. G. Peiffer

Corporate Research Science Laboratories, Exxon Research and Engineering Company, Clinton Township, Route 22 East, Annandale, New Jersey 08801

W. D. Dozier

Argonne National Laboratory, 9700 South Cass Avenue, Argonne, Illinois 60439

M. Y. Lin

National Institute of Standards and Technology, Route 117 and Quince Orchard Road, Gaithersburg, Maryland 20899

Received January 8, 1993; Revised Manuscript Received April 13, 1993

ABSTRACT: Two-dimensional light scattering and digital imaging studies of the structural evolution in a graft copolymer-homopolymer blend under quasi-static elongation are reported. The graft copolymer consists of a polydisperse elastomeric poly(ethyl acrylate) (PEA) backbone onto which monodisperse thermoplastic polystyrene (PS) chains are grafted. The homopolymer poly(ethyl acrylate) is produced in situ since grafts are not incorporated into every chain. The "quasi-equilibrium" structure of the graft copolymer blend cast from a good solvent exhibits isotropic scattering (i.e., appearance of a spinodal ring) with an inverse characteristic length $q_m \approx 4 \mu\text{m}^{-1}$. When the blend is subject to a quasi-static elongation ratio λ (=final length/initial length), three regimes are observed: (i) A transition regime at very low elongation ratios where the system behaves reversibly. (ii) A hyperelastic regime where the spinodal ring deforms in an anisotropic manner, i.e., ellipsoid-shaped scattering elongated in the direction perpendicular to the applied strain. The intensity $I_{\parallel}(q_z)$ parallel to the elongation increases in an exponential manner due to cooperative alignment of the hard PS-rich phase, and its peak position shifts in an affine manner to smaller values (i.e., $q_{zm} \sim \lambda^{-1}$). Moreover, the scattered light perpendicular to the elongation, $I_{\perp}(q_y)$, decreases in intensity as its peak position q_{ym} diverges to infinity. (iii) A plastic regime where $I_{\parallel}(q_z)$ remains nearly constant as its position q_{zm} converges to a finite value at $q_{zm} \approx 0.9 \mu\text{m}^{-1}$. In the three regimes, the structure factor parallel to the elongation, $S_{\parallel}(q_z)$, remains self-similar. The underlying mechanism of the deformation will be discussed within the framework of concentration fluctuations in "soft" elastic two-component solids.

I. Introduction

With the rapidly growing interest in multiphase polymers, knowledge of the interfacial characteristics at the phase boundary is taking on an ever-increasing importance in the scientific community.¹⁻³ In fact, the precise control of the interfacial region and its direct influence on the resultant morphology is a primary focus of research in this area of material science.^{4,5} Melt blending of available polymers is a convenient way to produce these multiphase materials.⁶⁻⁹ However, due to a vanishingly low entropy of mixing of the macromolecules, two demanding structural requirements have to be satisfied: (i) a controlled microphase separation in relation to a proper interfacial tension and (ii) an interphase adhesion strong enough to assimilate stress and strain without disruption of the established morphology. It is well established that, with appropriately-structured polymer compatibilizers, markedly improved physical properties are observed.¹⁰ These materials are typically block or graft copolymers in which segments of the chain interact in a favorable manner with each phase.¹¹ This "bridging" of the interfacial region enhances the interfacial adhesion and improves the dispersion and size of the discrete phase. The use of polymer compatibilizers is practically universal, and therefore a wide range of thermoplastic-thermoplastic, thermoplastic-elastomer, and elastomer-elastomer blends have been developed. In the majority of these blends, compatibilization occurs due to the formation (usually in situ, under reactive processing conditions) of graft copolymers.¹² Although the molecular structures of these copolymers are somewhat ill-defined, they are very effective in compatibilization at low concentrations since

their formation take places directly at the interface boundary.¹³

Besides their emulsifying effect, block and graft copolymers made of incompatible segments exhibit a variety of structures.^{14,15} The ability to undergo microphase separation and micellization endows block or graft copolymers with structures and properties not possessed by the parent homopolymers or their simple random copolymers.¹⁶ Examples include the well-known "thermoplastic-elastomer" poly(styrene-*b*-diene-*b*-styrene) which behaves as a thermoreversible cross-linked rubber due to the microphase separation of the glassy polystyrene end blocks.¹⁷ Surprisingly, very few morphological studies have been carried out on graft copolymers.¹⁶ The main reason appears to be the difficulty which exists in preparing reasonably well-defined graft copolymer systems. From the few studies that have been carried out, it appears that, depending on the number of grafts and uniformity in structure, graft copolymers can have domain morphology ranging from regular diblocks to segmented multiblock copolymers.¹⁸⁻²⁰ The preparation of suitable macromonomers and their subsequent use in the copolymerization with a low molecular weight monomer is the preferred method for preparing graft copolymers.²¹⁻²³

In this study, a family of graft copolymer-homopolymer blends was prepared. The former component consists of an elastomeric backbone of poly(ethyl acrylate) (PEA) with pendant monodisperse thermoplastic grafts of polystyrene, and the latter is the ungrafted elastomeric homopolymer. These components are immiscible and are therefore suitable candidates for probing the structure-property relationships of graft copolymer-homopolymer

blends which are very often prepared and described in the literature. Two-dimensional light scattering was used to follow the evolution of the structure under quasi-static elongation.

II. Experimental Section

Styrene monomer was initially purified by extensive washing with a 10 wt % sodium hydroxide solution and subsequently distilled under reduced pressure. *sec*-Butyllithium (Aldrich Chemical Co.) was used as received. Ethylene oxide (Eastman Kodak Co.), 1,1-diphenylethylene (Eastman Kodak Co.), ethyl acrylate, methyl ethyl ketone, and methacryloyl chloride (Aldrich Chemical Co.) were used as received. The methacrylate-terminated polystyrene macromonomers were synthesized by end capping anionically polymerized polystyrene anions with ethylene oxide and, subsequently, terminating the reactive group with methacryloyl chloride. The specific synthesis procedure is described by Milkovich et al.²⁴ The products were precipitated, washed with a large excess of methanol, and dried in vacuum for 48 h at 50 °C. The molecular weight and distribution were determined by gel permeation chromatography using tetrahydrofuran as the elution solvent with the instrument calibrated with monodisperse polystyrene standards.

¹H NMR was used to confirm the macromonomer end group. The macromonomer has an average molecular weight $M_w = 6900$ with a polydispersity $M_w/M_n = 1.2$. The poly(ethyl acrylate)-polystyrene based graft was synthesized by dissolving ethyl acrylate and the macromonomers (27 wt %) in methyl ethyl ketone and degassing with nitrogen gas for 2 h, while simultaneously heating the solution to 60 °C for 24 h. The polymerization was initiated with 2,2'-azobis(isobutyronitrile). The product was precipitated in a large excess of *n*-butanol and then extracted with a 50/50 decalin/petroleum ether mixture. The graft copolymer-homopolymer blend was dried in a vacuum oven for 24 h at 60 °C. This particular structure was synthesized because of the high degree of immiscibility between polystyrene and poly(ethyl acrylate). The styrene/ethyl acrylate composition was determined by elemental analysis and ¹H NMR. The number-average molecular weight of the graft copolymer as determined by GPC yielded $M_n = 175\,200$ g/mol. The average number of grafts per chain ($n = 7$) was estimated by $n = M_n W_{PS} / M_n^{(PS)}$, where $M_n^{(PS)}$ is the number-average molecular weight of the PS branch and W_{PS} is the weight fraction of the polystyrene component in the graft copolymer. The average molecular weight between grafts, estimated from M_n and $M_n^{(PS)}$, is approximately 15 900. The graft efficiency is about 97% as determined from GPC measurements using a combination of refractive index and ultraviolet detectors and extraction results. From these measurements, the product is found to contain approximately 20% by weight homopolymer. Relatively thick films (ca. 0.2 mm) were prepared by casting under a natural rate from a tetrahydrofuran (THF) solution at a 5 wt % total polymer concentration onto a Teflon-coated surface. The film was dried in a vacuum oven at 100 °C for 24 h and further annealed at 150 °C for 3 h before measurement. Rectangular pieces (3 × 0.5 cm) were cut from the sample.

The two-dimensional small-angle light scattering (SALS) experiments were performed using a two-dimensional 14-bit charge-couple device (CCD) detector (OMAIII from EG&G Princeton Applied Research). The incident light was a 0.5-MW He-Ne laser ($\lambda = 6328$ Å). The scattered light was detected by either one of the following methods: (i) The scattered light was made parallel with two large aperture lenses and subsequently collected on the CCD arrays (the geometry of the CCD was selected so that the entire scattering pattern could be observed); (ii) the scattered light impinges on a diffusive screen and is collected by a fixed gain video camera (Digital 5000, Panasonic) connected to an Image Grabber (Neotech Image Grabber NuBus, Neotech Limited and a Macintosh IIfx) and 8-bit digitized. The length scale that can be studied extends from $2\pi/q = 20$ to 0.95 μm , where $q = 4\pi/\lambda_0 \sin(\theta/2)$ is the scattering wave vector and λ_0 the wavelength in the scattering volume. Samples were uniaxially extended to a specific elongation ratio λ ($\lambda = L/L_0$, where L and L_0 are the stretched and unstretched lengths of the system) using a stretching device placed in the laser beam path.

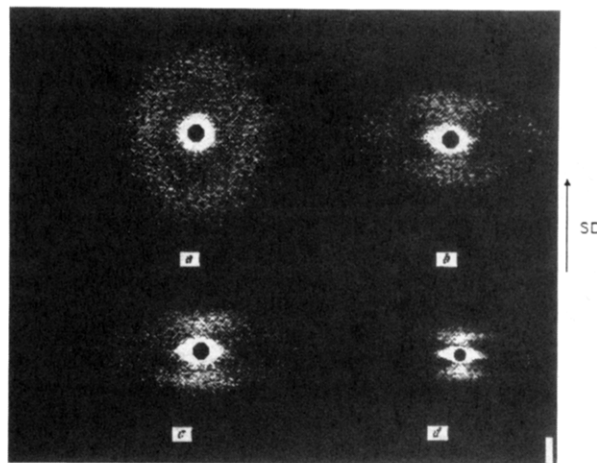


Figure 1. Two-dimensional SALS patterns for PEA-g-PS at various elongation ratios. The stretching direction is vertical, and the angle mark indicates 7°.

The sample was stretched to the desired elongation ratio and allowed to relax to the new stretched configuration for at least 10 min prior to data collection. All data were collected at room temperature and corrected for detector sensitivity, parasitic scattering, and background scattering. For clarity, a coordinate system O_{xyz} was established, with the axes O_x and O_y lying parallel to the propagation direction of the laser beam and the elongation direction, respectively. The SALS profile $I(q_y, q_z)$ was measured in the plane O_{yz} , where q_y and q_z are the O_y and O_z components of the scattering wave vector q .

III. Results and Discussions

A. General Trends. Figure 1 illustrates the evolution of the light scattering patterns for a series of elongation ratios ($\lambda = 1$ –4). The stretching direction is vertical. The general trends are fundamentally different when compared to the deformation of a homogeneous rubbery network. This is expected because of the inherently two-phase nature of the graft copolymer-homopolymer blend, i.e., hard polystyrene-rich domains in a rubbery poly(ethyl acrylate) (i.e., polystyrene poor) matrix. In the case of deformation of a homogeneous rubbery network, the scattering intensity should decrease relative to the isotropic case for q parallel to the stretching axis, as in all-chain orientation processes. The scattering intensity should exhibit a long axis perpendicular to the stretching direction. In the case of a microphase-separated system consisting of a "hard" minority region in a rubbery matrix, this normal anisotropy is expected to be at least partially masked at low q . The reason for this behavior is that the hard region simply deforms less than the elastomeric matrix. Upon elongation, the hard minority phase will phase separate in the direction parallel to the stretching direction. As a result, the graft copolymer-homopolymer blend is expected to be less homogeneous in this direction and the scattering intensity correspondingly increases at low q . In the perpendicular direction, the dimension of the sample is contracted due to the Poisson effect. The scattering intensity therefore decreases in this direction. We have classified the observed SALS patterns into three regimes (I–III) according to the specific elongation ratios.

In regime I (pattern a) corresponding to a very low λ ($\lambda = 1 + \epsilon$, $\epsilon \ll 1$), the graft copolymer exhibits an isotropic microstructure characterized by a nearly circular ring reminiscent of spinodal decomposition. This pattern indicates quasi-periodic concentration fluctuations with wavenumber q_m . The dominant characteristic length is about $2\pi/q_m = 1.2$ μm , and its periodicity does not depend on the elongation direction. In this regime, the system

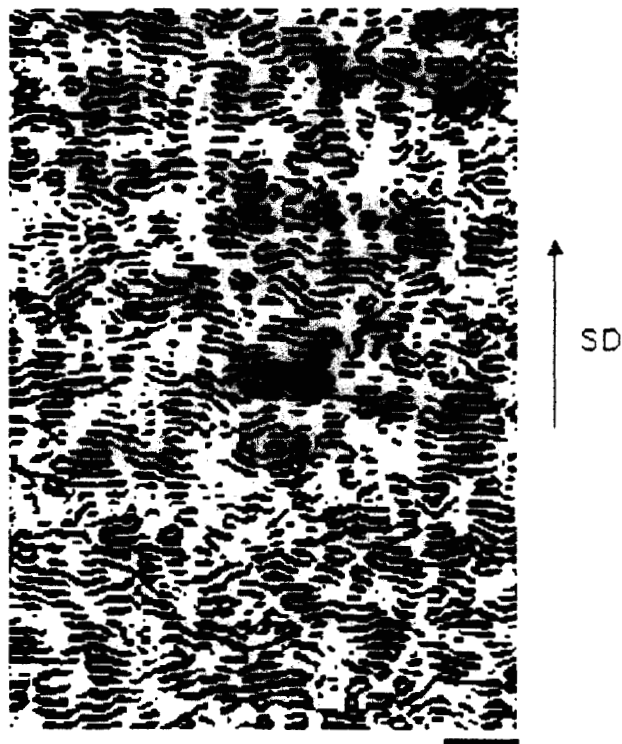


Figure 2. Phase contrast microscopy of the sample stretched at $\lambda = 4$, digitized with two intensity levels (black and white). The alignment of the PS-rich phase (black clusters) perpendicular to the stretching direction is clearly visible (the bar corresponds to 10 μm).

behaves reversibly because a slight deformation of the ring is almost immediately recovered upon releasing the stress.

In regime II (patterns b and c), corresponding to λ in the range 1.2–3.0, the isotropic light scattering pattern is progressively elongated in the direction normal to the stretching direction. The peak intensity parallel to the elongation, $I_{\parallel}(q_z)$, increases as its position shifts to smaller q . This scattering maximum implies that a pseudoperiodic structure with a spacing $2\pi/q_{zm}$ develops along the stretching direction. The peak intensity in the direction perpendicular to the stretching direction decreases in intensity as the magnitude of q diverges to infinity.

In regime III (pattern d) corresponding to $\lambda \geq 3$, the peak intensity converges slowly to an asymptotic value as its position remains constant up to the failure of the material at $\lambda \approx 5$. The dominant characteristic length in this regime is about 5 μm . This regime can be considered to be dominated by primary plastic deformation. Shown in Figure 2 is an optical micrograph of the sample stretched to $\lambda = 4$ (regime III). The periodicity of the fluctuations in the stretching direction is clearly visible as well as the alignment of the PS-rich phase perpendicular to the deformation axis. In the next section, we consider the effect of elongation on the SALS profile parallel to the stretching (i.e., $I(q_z) \equiv I(q_z, q_y = 0)$). The profile perpendicular to the stretching axis, ($I(q_y) \equiv I(q_z = 0, q_y)$), is also an interesting quantity but will be discussed in a future paper.

A prominent feature in the patterns a–c is the magnitude of the characteristic length ($>1 \mu\text{m}$). Typically, a well-defined graft copolymer is not expected to fluctuate on such a large length scale. The studies by Price et al.²⁵ on polyisoprene grafted on polystyrene have revealed a regular two-phase structure with a characteristic length of $\sim 100 \text{ \AA}$. On the other hand, graft copolymers synthesized by copolymerization of monomers and macromers exhibit

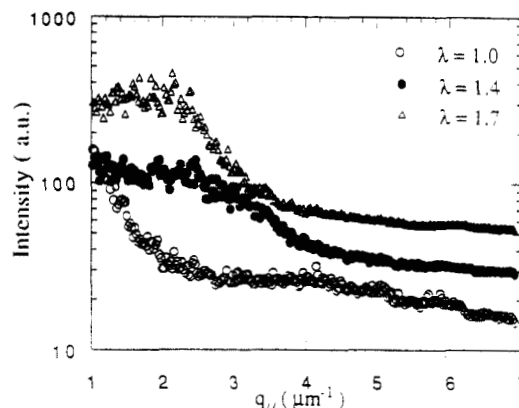


Figure 3. Profile of the scattering intensity $I_{\parallel}(q_z)$ along the stretching direction as a function of the scattering wave vector q_z .

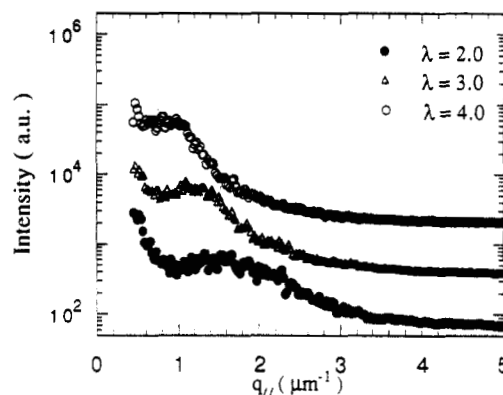


Figure 4. Profile of the scattering intensity $I_{\parallel}(q_z)$ along the stretching direction as a function of the scattering wave vector q_z .

correlation lengths on the order of microns as shown by Maeda and Inoue.²⁶ The reasons for such large-scale fluctuations are numerous: (i) a distribution of backbone segment length or molecular weight between graft macromers; (ii) the inevitable presence of homopolymers deficient in graft due to the difference in the feed ratios of the starting monomers as well as their reactivity ratios [in this study, the feed ratios between the mole fraction of macromers and monomers (M_1/M_2) are approximately equal to 0.003 and their reactivity ratios $r_2 \approx 0.724$]; (iii) polydispersity of the graft copolymers. The magnitude of these effects and how each contributes to affect the final structure is beyond the scope of the present paper and will be discussed in a future paper. Our preliminary studies, as noted previously, indicate that a moderate amount of homopolymer is present in the product.

B. Change in the Scattering Profile with Elongation. B1. Results. Figures 3 and 4 show the typical evolution of the light scattering intensity parallel to the elongation at different values of λ . The relative intensity $I_{\parallel}(q_z)$ was plotted as a function of the scattering vector. These figures clearly show that a single scattering maximum appears at a finite value of q . The peak height increases with λ and the peak position q_{zm} shifts to a lower value reflecting a "pseudo-coarsening" which is reminiscent of the late stage of a spinodal decomposition process. In addition, the breadths Δq (full width at half-maximum) of the scattering curves which reflect the distribution of correlation lengths become significantly narrower with λ . The peak width Δq as a function of elongation is plotted in Figure 5. A fit to the curve with a scaling law of the form $\Delta q \propto \lambda^\omega$ results in a value of $\omega = -1.3$. Figure 6 shows the plot of the maximum intensity I_{zm} vs λ . The inset in

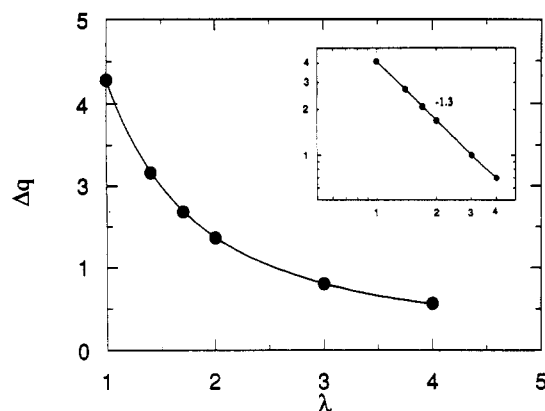


Figure 5. Full width at half-maximum of the scattering intensity $I_{\parallel}(q_z)$ curves as a function of the elongation ratio λ .

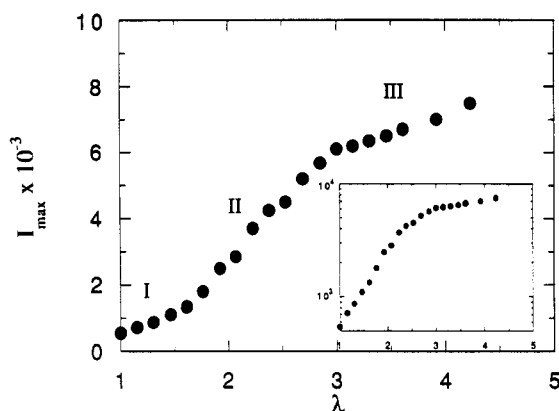


Figure 6. Evolution of the maximum intensity as a function of λ , showing three distinct regimes. The inset displays the semilogarithmic plot showing the exponential behavior of I_{\max} .

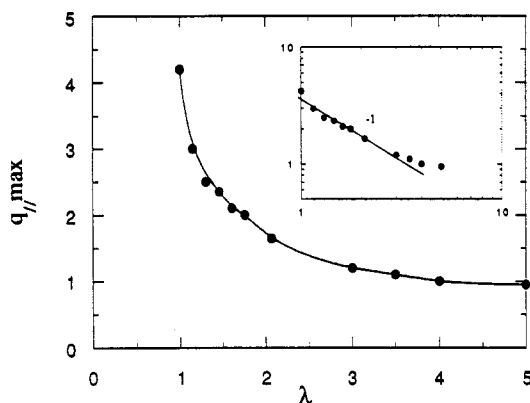


Figure 7. Evolution of the inverse of the correlation length as a function of the elongation ratio λ . The inset is the log-log plot showing affine deformation.

Figure 6 is the semilogarithmic plot of I_{zm} vs λ . The maximum intensity increases linearly in regimes I and II and then reaches an asymptotic value in regime III. The straight line behavior represents an exponential growth of the fluctuations, again reminiscent of the dynamics of spinodal decomposition. In the following discussion we show qualitatively that this exponential growth is due to a *cooperative alignment* of the PS-rich domains perpendicular to the elongation direction. Finally, the position of the peak q_{zm} as a function of λ is plotted in Figure 7. Clearly, an affine deformation is observed up to the regime II, i.e., $q_{zm} \propto \lambda^{-1}$. The isochoric affine deformation predicts that the measured scattered intensity profiles, $I(q_z)$, should be universal and superimposable to each other if I is plotted as a function of the reduced scattering vector q/q_m . This reduced plot is presented in Figure 8. The curves are not

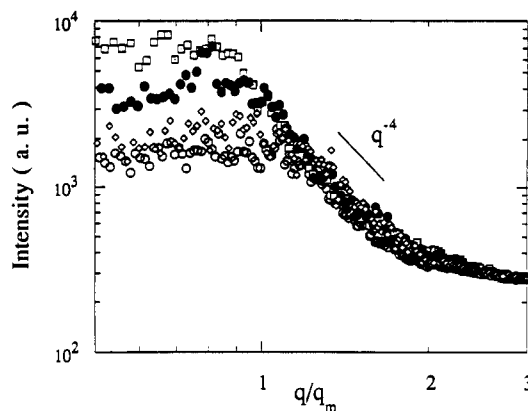


Figure 8. Scattered intensity profile as a function of the reduced scattering wave vector.

superimposable as the peak intensity increases with λ . The elongation therefore involves an additional mechanism beyond that suggested by the single affine deformation. At high q/q_m , the curves are consistent with a q^{-4} scaling as one would see with Porod interfacial scattering.

B2. Discussion. In the copolymerization of macromer/monomer systems, the concentration of the starting macromer is generally very low because of its high molecular weight (see the Experimental Section). To ensure a maximum conversion of the macromers, the reaction is usually conducted beyond 50% of the total monomer conversion. As a result, the polydispersity of the graft copolymers increases and a moderate amount of homopolymer (i.e., copolymers deficient in grafts) is present in the final product. The equilibrium structure of the system is therefore a complex combination of micellization of the graft copolymer, emulsification of the homopolymer by the graft copolymers, and "macrophase" separation between the homopolymers and the graft copolymers. Nevertheless, the possible mechanism of the evolution of the structures in these systems can be detailed. In order to exhibit fluctuation on a length scale on the order of microns, the dominant mechanism has to be a macrophase separation between the homopolymers (along with the PS-poor graft copolymers) and the PS-rich graft copolymers. Recent TEM and SANS measurements seem to confirm this picture.²⁷ A macrophase separation between PS-rich graft copolymers (minority phase) and PS-poor graft copolymers has one very important consequence: the "hard" minority region rich in PS is now embedded in a rubbery matrix of PEA which is *inhomogeneous* in elasticity because of the presence of the homopolymers. When the sample is cast from a nonselective solvent (such as tetrahydrofuran), an interconnected network of PS-rich domains is observed which persists through the annealing of the sample (see the isotropic light scattering pattern in Figure 1a). The dispersion of the correlation lengths between the PS microdomains is quite broad as seen from Figure 5. During the microphase separation it is likely that the homopolymers will be expelled from the PS microdomains. It is reasonable therefore to expect their concentration to be higher in the interstitial regions with the lowest correlation length in the distribution. Consequently, those regions will be more elastomeric than the average (see Figure 9). When the sample is stretched, the regions with the higher concentration of elastomeric homopolymer are expected to deform more rapidly than the homopolymer-poor regions. It appears that this is the mechanism underlying the alignment of the PS-rich regions.

In summary, when the graft copolymer system is subject to elongation, two processes take place: (i) the PS-rich

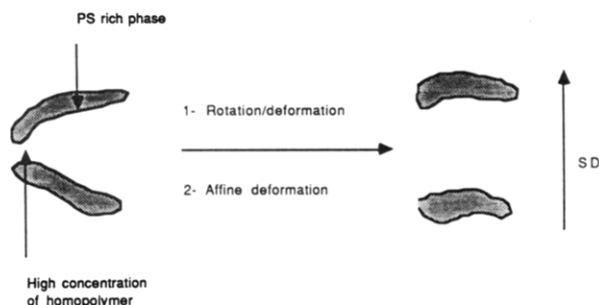


Figure 9. Schematic drawing showing the cooperative rotation and alignment of the PS-rich phase perpendicular to the stretching direction.

regions are elongated (as noted by the appearance of the ellipsoid anisotropy (see Figure 1b)); (ii) the region rich in homopolymer will be the first to elongate. This causes a *cooperative rotation* of the PS-rich phase, leading to an increase in the scattering intensity parallel to the elongation direction (see Figure 6). The overall response of the material is still affine, as shown in Figure 7.

IV. Conclusion

A graft copolymer–elastomeric homopolymer blend was synthesized, with the former component containing an elastomeric backbone onto which a low level of thermoplastic components are grafted. The two segments of the chains are immiscible and, as a result, are able to form phase-separated regions of the thermoplastic (minor component) in an elastomeric matrix (major component). Since this type of graft copolymer–homopolymer blend is highly useful as a thermoplastic–elastomer or as a polymer blend compatibilizer, the structure of this material was probed using two-dimensional light scattering under both quiescent and strained conditions.

The results clearly show that the dispersed phase (e.g., polystyrene grafts) phase separates from the matrix under quiescent conditions. Furthermore, as the material is elongated (i.e., as in conventional stress–strain measurements), the phase-separated regions respond to the stress by orienting perpendicular to the stretching direction. Qualitatively, this response resembles the observations on a semicrystalline polymer subject to elongation.²⁸ At low elongation ratios, the graft copolymer–homopolymer blend responds reversibly. However, the response becomes irreversible at higher elongations. In fact, the light scattering measurements show that three distinct regimes of structure “modification” are observed. Prior to plastic deformation, the blend responds to the deformation in an affine manner. This is interpreted as being due primarily to the elastomeric nature of the matrix material. These results should lead to a better understanding of the structure–property relationships of graft copolymer–

homopolymer systems and, in addition, may be useful for understanding the behavior of these materials in such systems as in binary component blends. These studies have been initiated and will be reported in a later publication.

Acknowledgment. M.R. thanks Scott Milner for fruitful discussions. The work at Argonne was performed under the auspices of the U.S. Department of Energy, Division of Material Science, Office of Basic Energy Sciences, under Contract W31-109-ENG-38. Support for W.D.D. by NSF Contract No. DMR-8902024 is gratefully acknowledged.

References and Notes

- (1) Bucknall, D. G.; Higgins, J. S.; Penfold, J. *Physica B* **1991**, *180* & *181*, 468.
- (2) Shull, K. R.; Kramer, E. J.; Hadzioannou, G.; Tang, W. *Macromolecules* **1990**, *23*, 4780.
- (3) Leibler, L. *Physica A* **1991**, *172*, 258.
- (4) Brown, H. R. *Macromolecules* **1989**, *22*, 2859.
- (5) Shull, K. R.; Kramer, E. J. *Macromolecules* **1990**, *23*, 4769.
- (6) Walsh, D. J.; Higgins, J. S.; Macconnachie, A. *Polymer Blends and Mixtures*; Nato Advanced Study Institute Series E89; Applied Science: New York, 1985.
- (7) Paul, D. R. In *Polymer Blends*; Paul, D. R., Newman, S., Eds.; Academic Press: New York, 1978; Vol. 2, p 35.
- (8) Olabisi, O.; Robeson, L. M.; Shaw, M. R. *Polymer–Polymer Miscibility*; Academic Press, Inc.: New York, 1979.
- (9) Gaylord, N. G. *J. Macromol. Sci., Chem.* **1989**, *A26* (8), 1211.
- (10) Corner, T. *Adv. Polym. Sci.* **1984**, *62*, 95.
- (11) Fayt, R.; Jerome, R.; Teyssie, P. *Makromol. Chem.* **1986**, *187*, 837.
- (12) Xanthos, M.; Dagli, S. S. *Polym. Eng. Sci.* **1991**, *31*, 929.
- (13) Song, Z.; Baker, W. E. *J. Appl. Polym. Sci.* **1992**, *44*, 2167.
- (14) Bates, F. S. *Science* **1991**, *251*, 898.
- (15) Aggarwal, S. L. *Block Copolymers*; Plenum Press: New York, 1970.
- (16) Brown, R. A.; Masters, A. J.; Price, C.; Yuan, X. F. In *Chain Segregation in Block Copolymers*; Comprehensive Polymer Science: Booth, C., Price, C., Eds.; 1989; Vol. 2, p 155.
- (17) Holden, G.; Bishop, E. T.; Legge, N. R. *Thermoplastic Elastomers*, Proceedings of the International Rubber Conference, 1967; MacLaren and Sons: London, 1968, p 287.
- (18) Chem-Tsai, C. H.; Thomas, E. L. *Macromolecules* **1981**, *22*, 333.
- (19) Price, C.; Lally, T. P.; Watson, A. G.; Woods, D.; Chow, M. T. *Br. Polym. J.* **1972**, *4*, 413.
- (20) Evans, D. C.; George, M. H.; Barrie, J. A. *Polymer* **1975**, *16*, 690.
- (21) Rempp, P. F.; Franta, E. *Adv. Polym. Sci.* **1984**, *58*, 1.
- (22) Kazanskii, K. S.; Kubisa, P.; Penczyk, S. *Russian Chem. Rev.* **1987**, *56* (8), 777.
- (23) Meijs, G. F.; Rizzardo, E. *Rev. Macromol. Chem. Phys.* **1990**, *C30* (3 & 4), 305.
- (24) Schulz, G. O.; Milkovich, R. *J. Polym. Sci., Polym. Chem. Ed.* **1984**, *22*, 1633.
- (25) Price, C.; Singleton, R.; Woods, D. *Polymer* **1974**, *15*, 117.
- (26) Maeda, M.; Inoue, S. *Makromol. Chem., Rapid Commun.* **1981**, *2*, 537.
- (27) Dozier, W.; Lin, M. Y.; Peiffer, D. G.; Rabeony, M., in preparation.
- (28) Wilke, W.; Bratrich, M.; Heise, B.; Peichel, G. *Polym. Adv. Technol.* **1992**, *3*, 179.